The International Journal of

ENERGY & ENGINEERING SCIENCES

GAZIANTEP UNIVERSITY

January, 2017
Issue: 1
Volume: 2

Energy Systems Engineering Publications
Gaziantep University, TURKEY

Editor In Chief Asst. Prof. Dr. Adem Atmaca
Co-Editor Asst. Prof. Dr. Nihat Atmaca

Gaziantep University Engineering Faculty
+90 342 360 12 00
+90 342 360 10 13
gaziantep.university.ijees@gmail.com
https://uemk-conferences.wixsite.com/ijees

Published by

Gaziantep university, Engineering Faculty, Energy Systems Engineering, Üniversite Bulvarı 27310 Şehitkamil - Gaziantep, TÜRKİYE

ISSN

Table of Contents

ASSESSMENT OF ENERGY MANAGEMENT IN FEED PLANTS: A REVIEW OF NECESSITY AND OBJECTIVE

Fatih BALCI
Assist. Prof. Dr. in Department of Energy Systems Engineering in Gaziantep University
fbalci@gantep.edu.tr

ABSTRACT: Energy demand, especially in the industrial sector, is rapidly increasing in our country. Due to the inadequacy of energy production to meet demand and the limit of new energy sources, it is becoming compulsory to import energy. This demonstrates the necessity of more efficient use of energy in all sectors. The energy sector is used intensively in the industrial sector and the highest consumption values are achieved according to other sectors. For this reason, it has become a necessity to attach importance to energy management and energy efficiency in the industry. Energy use is an important issue in the feed plants. Over the past decade, the significant increase in energy costs has contributed to reducing plant profit margins. Since profit margins are generally relatively low in wheat processing plants, efficient management of energy consumption has become a necessity instead of preference. A better efficient utilization of fuel, electricity, thermal energy and labor are the major components of manufacturing cost in feed plants.

INTRODUCTION

Increasing the usage will increase the cost of product directly as well as the reduction in the total margins of the plant. Energy prices doesn't seems to be reduced in the near future. Therefore, energy management system and recovery of energy, where applicable, must be applied to decrease the energy consumption and the increase in the margins. On the other side, current/prospective environmental legislations and concerns over the environment to increase industrial energy efficiency. Manufacturers prefer to use the most cost-effective techniques to increase energy efficiency in their plants.
In feed plants, the energy consumption is very high. Each process consumes generally more energy than it needs. The optimum energy supply must be calculated. Sometimes higher energy level will be needed depending on the type of raw material and the flow rate. Commercially available energy management systems can collect energy data using one or more parameters and they can be used to identify opportunities for daily energy. They can be used with a range of sensor technologies to monitor energy carried by electricity and gas as well as other energy carriers. They can analyze these data to separate energy use resulting from production schedules from that which is driven by the weather. They can be used to target process, plant or site efficiency improvements and to display information at a range of levels from shop floor to stakeholder's level. However,

these systems suffer from lack of standardization and real-time automatic correlation of energy data across multiple production levels. Existing EMS have been shown to reduce energy use by 5% (Carbon Trust, 2008).

Another way to improve the energy and resource efficiency of manufacturing processes is the recovery of waste streams and heat losses. Energy conservation is vital for the sustainability of the feed plants. Reduced energy consumption through conservation can benefit not only energy consumers by reducing their energy costs but also the society in general by reducing the use of energy resources and the emission of many air pollutants such CO_2 (Wang, 2014).

New technologies in mixed feed production ensure safe feed production while increasing the amount of energy consumed per unit product due to high energy consumption (Figure 1). Reducing or constantly controlling the burden of energy costs within mixed feed costs is gaining importance day by day in a competitive sector.

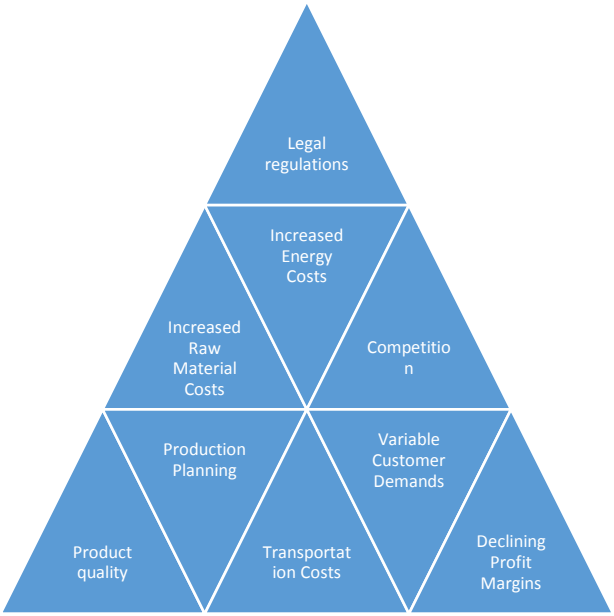

Figure 1. Main cost items in feed plants

Energy use is one of the important factors that have an impact on mixed feed production costs (Figure 2). Electricity and steam energy are heavily consumed in mixed feed production processes. Steam is mainly used in the pellet stage after powder feed production, while it is extensively used throughout the electric product processing stages. In addition, pressurized air is among the types of energy required to operate some transport and lock mechanisms. For this reason, the production methods have a separate precaution in terms of mixed feed quality. One of the ways to minimize energy consumption is to optimize the use of machinery in production without compromising feed quality. For this reason, an energy management system should be installed in each mixed feed factory and energy use should be monitored continuously.

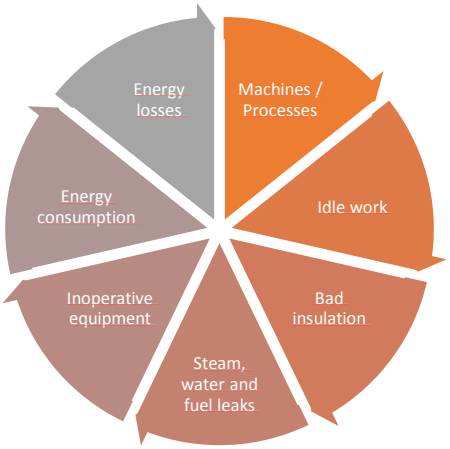

Figure 2. Aspects of energy management in feed plants

Energy management has not been considered as a vital issue so far compared with others such as production planning, marketing and the quality of product which thought a higher priority in the plant. The amount of energy used in the feed plant is an important economical consideration. Energy management is becoming a key skill in the manufacturing operations of many companies. Existing solutions for measurement, analysis and control of energy do not address all the requirements of energy management at the organization, factory or process level because they do not adequately develop in the workforce an awareness of the energy used in their business. Conventional energy management methods at the factory floor are limited because the energy performance of individual processes cannot be understood without continuous measurement of energy consumption and an infrastructure to map process energy data onto relevant business performance measures (Figure 3).

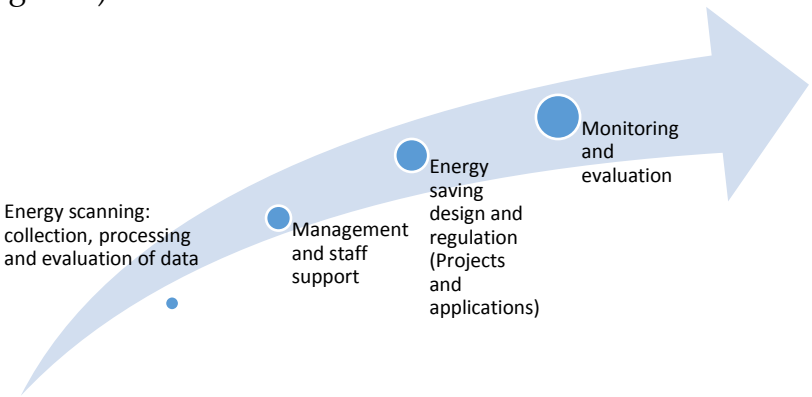

Figure 3. Energy Management Systems in Production Facilities

Each process, motor, pump, roll, machine etc. must be monitored according to their flow rate and energy consumption daily base. Also, the data should be interpreted into a meaningful directive to the operators. The fluctuations of energy usage, on the other hand, must be monitored by the data. Thus energy management for a plant must be unique for the successful implementation. Electric energy is a crucial factor in global industrial production. It can be saved

the unnecessary energy consumption by having a definite control of flour mill maintenance plan, minimizing process time and cutting down the maintenance expenses. Having a complete control of energy usage of each process is the main step of energy saving. High efficiency motors reduce energy losses through improved design, better materials and tighter tolerances and improved manufacturing techniques. Poor motor cooling can increase motor temperature and winding resistance, shortening motor life, in addition to increasing energy consumption. In addition to energy savings, this can help avoid corrosion and degradation of the system.

As a summary, effective energy management in production is a need towards increased energy efficiency in feed production plants. In order to reduce energy consumption and costs it is essential to use energy management during especially in pelleting process.

REFERENCES

Akdeniz, R. C. ve Boyar, S., 2002, Karma Yem Üretim Makinalarının Uygun Kullanımı. 2002 Yılı Hayvancılık Grubu Bilgi Alışverişi Toplantısı Bildiri Kitabı, T. C. Tarım ve Köyişleri Bakanlığı Ege Tarımsal Araştırma Enstitüsü Müdürlüğü, Yayın No: 106, Menemen /İzmir, s:147-166.

Akdeniz, R. C., Ak, İ. ve Boyar, S.,2005, Türkiye Karma Yem Endüstrisi ve Sorunları. VI. Türkiye Ziraat Mühendisliği Teknik Kongresi. TMMOB Ziraat Mühendisleri Odası (ZMO) 03-07 Ocak 2005, Cilt:2, Ankara, s.935-959.

Boyar, S. 2006. A Research on Determination and Development Possibilities of Energy Efficiency in Mixed Feed Industry (Case studies in two factories). Ph.D. Thesis, Agricultural Machinery Dept., Institute of Natural and Applied Sciences, Ege University, Bornova, Izmir, 416 p.

Boyar, S., Hepbasli, A., & Akdeniz, R. C. (2012). Energy utilization needs in Turkish mixed feed industry. Journal of Food, Agriculture & Environment, 10(3&4), 528-533.

Bunse, K., Vodicka, M., Schönsleben, P., Brülhart, M., & Ernst, F. O. (2011). Integrating energy efficiency performance in production management–gap analysis between industrial needs and scientific literature. Journal of Cleaner Production, 19(6), 667-679.

Carbon Trust (2004) Food and Drink Fact Sheet, GIL149, London, The Carbon Trust available from; www.carbontrust.co.uk/publications.

Carbon Trust, 2008. Automatic Monitoring and Targeting Equipment: A Guide to Equipment Eligible for Enhanced Capital Allowances. Report number ECA756, available from: www.carbontrust.co.uk (accessed 04.012.16)

Ergül, M., 1994, Karma Yemler ve Karma Yem Teknolojisi. Ders Kitabı. Ege Üniversitesi Ziraat Fakültesi Yayınları No:384. II. Basım. Bornova- İzmir, 280s.

Kedici Ö. Fizik Yük. Müh. "Enerji Yönetimi" Elektrik İşleri Etüd İdaresi Genel Müdürlüğü Enerji Kaynakları Etüd Dairesi Başkanlığı 1993 Ankara

SÖĞÜT, Z., & OKTAY, Z. SANAYİ SEKTÖRÜNDE ENERJİ TARAMASININ ENERJİ VERİMLİLİĞİNE ETKİSİ VE BİR UYGULAMA.

Swat, M., Brünnet, H., & Bähre, D. (2014). Selecting manufacturing process chains in the early stage of the product engineering process with focus on energy consumption. In Technology and Manufacturing Process Selection (pp. 153-173). Springer London.

Wang, Lijun, Weller, Curtis L, Jones, David D, & Hanna, Milford A. (2008). Contemporary issues in thermal gasification of biomass and its application to electricity and fuel production. Biomass and Bioenergy, 32(7), 573-581.

Wang, Lijun. (2014). Energy efficiency technologies for sustainable food processing. Energy efficiency, 7(5), 791-810.

Warechowska, Małgorzata. (2014). Some physical properties of cereal grain and energy consumption of grinding. Agricultural Engineering, 1(149), 239-249.

Xenergy, Inc. 1998. United States Industrial Electric Motor Systems Market Opportunities Assessment. U.S. Department of Energy's Office of Industrial Technology and Oak Ridge National Laboratory.

ON THE ENERGY STORAGE SITES FOR NATURAL GAS: AN OVERVIEW FOR TURKISH CASE AND REGULATION

Hamza GÜLLÜ
University of Gaziantep, Department of Civil Engineering
hgullu@gantep.edu.tr

ABSTRACT: It is aimed in this paper to mention about underground storage of natural gas. For this purpose, Tuz Lake underground natural gas storage project and Turkish regulation (UNGSP, 2011) have been overviewed. It is understood from the study that the project (Tuz Lake underground natural gas storage) presents new insights for the natural gas storage. However, investigation about the flow characteristics (rheology) during drilling of salt deposit is offered for better design. The Turkish regulation (UNGSP, 2011) is found to involve with the storage plant in the management viewpoint rather than technical issues. Thus, alternately a new regulation in technical viewpoint dominantly can be useful for the natural gas storage operations.

Key words: energy, natural gas, storage

INTRODUCTION

Energy storage of natural gas becomes one of primary issues of energy politics when the country imports the gas mandatory. Specifically for excessive amount of gas, the requirement of storage becomes more important by considering in the viewpoint of engineering structure, as well as characteristics of soils and rocks under complex and extreme conditions that offer mechanical, hydraulic and geotechnical processes in order for developing analytical tools and methods. In many of energy storage systems, it has been know that cyclic charging and discharging will occur with a known time scale. Energy storage of natural gas could be in different forms particularly in subsurface. Opportunities to store thermal heat energy in salt domes in the form of thermohaline reservoirs is considered an alternative approach (Wuttke et al., 2014), which could be a good candidate for the storage of natural gas. This could also provide sustainable solutions for the energy requirements of country. During the subsurface storage of natural gas, permeability enhancement of rock deposits could be a viable issue via hydraulic fracturing. It could be offered that energy storage for natural gas applications may include the underground spaces in salt caverns or aquifers, or as well as the energy storage in the form of compressed gas in caverns or aquifer (McCartney et al., 2016).

It is reported that there are several applications in engineering practice related to operations in the energy sector that requires new developments. They can be

summarized as pipeline construction, design of foundation systems for offshore wind or tidal energy, mining operations related with oil sands, design of dams for hydro energy storage, and quantification of embodied energy in geotechnical infrastructures, etc. Moreover, in a variety of applications specifically in the geotechnical viewpoint, geosynthetic-reinforced retaining walls, energy piles, tunnels and diaphragm can utilize the ground for heating and cooling of structures, storage of heat, or dissipation of waste heat. Main issues within those applications could be considered to understand the coupled role and the mechanical response of the media (i.e., changes in strength, volume change, changes in stiffness) to predict the flow of fluids, transfer of heat in porous or fractured media, etc. The governing equations for the heat transfer and water flow for water-saturated porous media are well researched in the literature. However, the issues above could also present new insights for civil engineers in terms of technical problems associated with soil-structure interaction (McCartney et al., 2016).

It is aimed in this paper to mention about underground storage of natural gas for energy use. For this purpose, Tuz Lake underground natural gas storage project (Turkey) has been overviewed with present Turkish regulation (UNGSP, 2011).

TUZ LAKE UNDERGROUND NATURAL GAS STORAGE PROJECT AND SOME DISCUSSIONS

A typical description of Tuz Lake underground natural gas storage project has been illustrated in Fig.1. In summary, the salt deposit underground nearly in the depth greater than 700m in Sultanhanı (Aksaray) 40km away from Tuz Lake is attempted to be melted via the clean water supplied from Hirfanlı Dam 120km away. After melting the salt deposit, caverns for natural gas storage are aimed to be constructed. Then, the melted salt is transferred and discharged into Tuz Lake through 40km pipe line. For storage of natural gas, 12 caverns are planned to construct with the volume of nearly 600000m^3 for each. It is reported that Turkey has a consumption of 40 billion m^3 natural gas per year. After completing the 12 caverns within the salt mass for natural gas storage, it is offered that nearly 1 billion m^3 natural gas will be stored per year. This means that Turkey will have 2.1 billion m^3 natural gas storage capacity together with Silivri Plant (having the capacity of 1.1 billion m^3 natural gas). This provides a guarantee for 5% of total natural gas consumption of country (Energy Institution).

It is reported that the natural gas could be alternately stored in hard rock caverns, aquifers, old mine sites, in the consumed reservoirs of oil and gas, as well as salt caverns. But it can be said that for Turkey Tuz Lake site presents new insights in the storage viewpoint for future studies involving engineering structures. However, there may be some querying with relevant discussions about the project (Fig.1) involved with the issues of water supply, drilling operations of salt deposit for caverns and discharge of melted salt into Tuz Lake. The feasibility studies

indicate that Hirfanlı Dam seems relatively sufficient for water supply for melting salt during the storage operations. The supplied water is reported as %1.22 of total volume of Hirfanlı dam reservoir (Botaş, 2017). This can be accepted as a relatively minor effect for the dam use. However, the distance 120km away for water supply could be queried in the economy viewpoint. On the effect of melted water discharged into Tuz Lake 40km away from salt deposit, it is reported that (Botaş, 2013) the melted water will contribute to Tuz Lake that is under the threat of evaporation and aridness. Since the melted water will be discharged inside Tuz Lake (not directly to surface), it is not expected adverse effect on the water surface of lake. As for the operation of drilling of salt deposit for obtaining storage caverns, some technical queering could be useful for optimum drilling. For the structural design within the queering, it could be important to investigate the issues of flow characteristics (rheology) of salt+water mass, drilling velocity, pumping velocity, pumping pressure, flow rate, etc. One more important issue during the storage of natural gas could be considered as the environment protection. For this issue, it is reported (Botaş, 2013) that effect of environmental problems (wastewater, solid waste, noise pollution, ecological impact, use of blasting materials, seepage of boring sludge into groundwater, disposal of boring sludge, etc.) will be in minor level that provides the project of Tuz Lake natural gas storage being friendly environment.

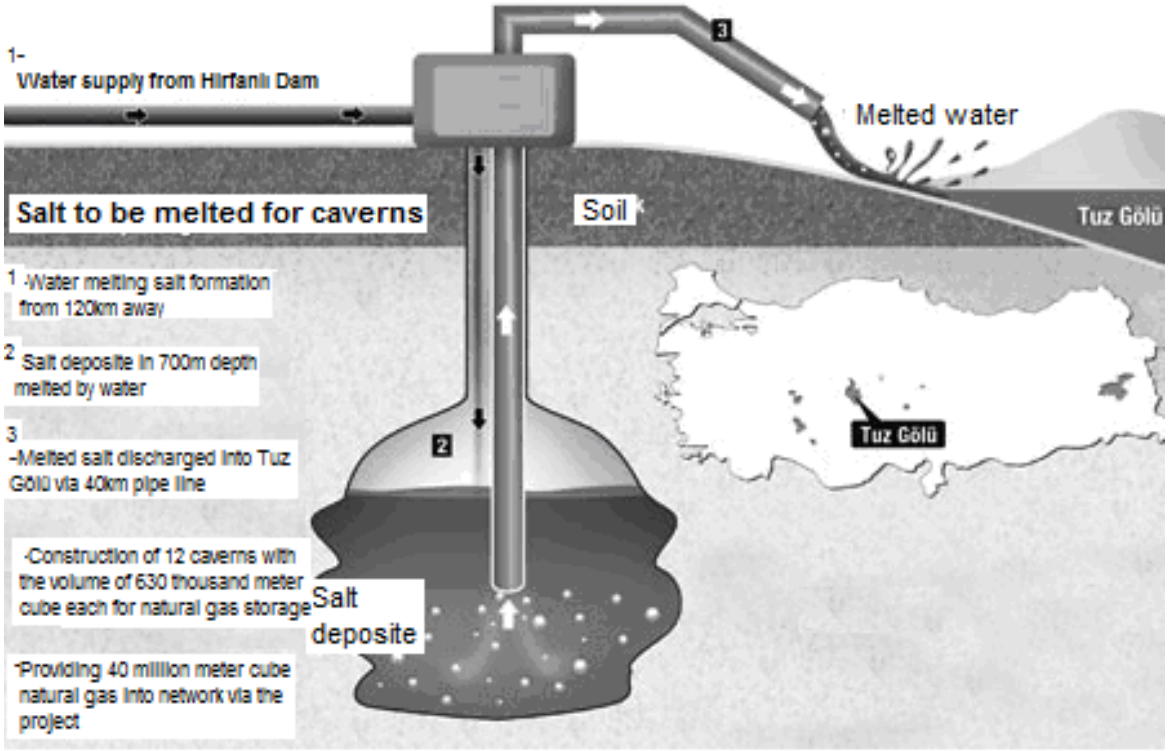

Figure 1. A Typical Description of Tuz Lake Underground Natural Gas Storage Project (Energy **Institution, 2017)**

A TURKISH REGULATION FOR UNDERGROUND NATURAL GAS STORAGE PLANT

A Turkish regulation (UNGSP, 2011) was published by Republic of Turkey Energy Market Regulatory (T.C. Enerji Piyasası Düzenleme Kurumu) for the fundamentals of underground natural gas storage plant. Highlights of some fundamental points could be summarized as follows:

-The company of Natural Gas Storage Plant serves in accordance with related codes and regulations (Pr or Provision 5.2).
-In the cases of security risk for natural gas storage plant or network and restoration or maintenance of plant, there could be power cut or reduction by the company (Pr.9.1).
-The company of storage plant is responsible for operating natural gas system in safe and efficiency (Pr.11.1).
-The company should conduct the maintenance and restoration works without power cut or reduction in storage servings. However, in mandatory cases of power cut or reduction due to the maintenance and restoration, the power cut and reduction should be equally reflected to the clients (Pr.14.1).

As understood from the regulation UNGSP (2011) highlighted above, the provisions of the regulation is mostly related with management operations of storage plant. It can be said that there are missing considerations or indirect points in the regulation (UNGSP, 2011) in the technical viewpoints when considered Tuz Lake natural gas storage project Thus, UNGSP (2011) should be discussed with an extension, or alternately a new regulation should be prepared by more technical provisions in the viewpoint of engineering structure. In view of this, it is recommended some provisions for the natural gas storage operations including water supply for melting, drilling of salt deposit for storage cavern and discharge of melted water into environment.

CONCLUSION

From the study in this paper, it can be concluded that drilling operations of salt deposit (Tuz Lake underground natural gas storage project) needs rheological investigations for optimum design. In addition, the present Turkish regulation (UNGSP, 2011) is found a lack of technical issues of storage that could be offered for future regulations.

RECOMMENDATIONS

Flow characteristics of salt deposit during drilling operation (Tuz Lake underground natural gas storage project) could be investigated for better design. The present Turkish regulation (UNGSP, 2011) could be improved with more

technical issues, or a new regulation including technical issues could be prepared for underground natural gas storage.

REFERENCES

Botaş. (2013). Tuz Gölü Doğal Gaz Yeraltı Depolama Projesi Çevre Yönetim Planı. Çınar Mühendislik Müşavirlik A.Ş. Retrieved on October 01, 2017 from http://documents.worldbank.org/curated/en/752081468318870399/pdf/E4152v40Turkey00110201300Box374358B.pdf.

Botaş. (2017). Tuz Gölü Yeraltı Doğal Gaz Depolama Tesisi Kapasite Artışı Projesi. Çınar Mühendislik Müşavirlik A.Ş. Retrieved on October 01, 2017 from http://documents.worldbank.org/curated/en/190631496821940999/pdf/SFG3412-EA-TURKISH-P162727-Box402913B-PUBLIC-Disclosed-6-7-2017.pdf.

Energy Institution. Retrieved on October 02, 2017 from http://enerjienstitusu.com/2011/11/20/cinliler-tuz-golunde-ikinci-buyuk-dogalgaz-deposunu-insaa-edecek/

McCartney, J.S., Sánchez, M., Tomac, I. (2016). Energy geotechnics: Advances in subsurface energy recovery, storage, exchange, and waste management. Computers and Geotechnics, 75, 244–256.

UNGSP (Turkish Regulation for Fundamentals of Underground Natural Hazard Storage Plant). (2011). Yer Altı Doğal Gaz Depolama Tesisi Temel Kullanım Usul Ve Esaslarının Belirlenmesine Dair Yönetmelik. Enerji Piyasası Düzenleme Kurumu, Resmi Gazete, Sayı: 27954. Retrieved on October 02, 2017 from www.epdk.org.tr/TR/Dokuman/3459.

Wuttke, F., Wagner, N., Khan, M., Thess, A., Scherzber, H. (2014). Thermohaline energy geo-storage: evaluation of fluid–fluid layer and fluid-rock salt evaluation. Géotech Lett, 4:132–8.

AN ALTERNATIVE METHOD FOR THE SUN DRYING OF TRADITIONAL DRIED EGGPLANT

Ghaith Al-QUDSI[1], Ezgi YAYVAN[3], Fatih BALCI[2*], Mustafa BAYRAM[3]

[1]Gaziantep University, Faculty of Natural and Applied Science, Department of Biochemical Science and Technology, 27310 Gaziantep/Turkey
[2]Gaziantep University, Faculty of Engineering, Energy Systems Engineering, 27310 Gaziantep/Turkey
[3]Gaziantep University, Faculty of Engineering, Department of Food Engineering, 27310 Gaziantep/Turkey
***Corresponding author: fbalci@gantep.edu.tr**

ABSTRACT: Eggplant (Solanum melongena L.) is an important market vegetable of Asian and Mediterranean countries. According to Food and Agriculture Organization of the United Nations, world production of eggplants was around 50.19 million tons in 2014. China as main producer (29.5 million tons) followed by India (13.5 million tons), Egypt (1.2 million tons), Iran (0.85 million tons) and Turkey (0.82 million tons) (FAO, 2014). Turkey is one of the worlds largest growers, whose annual production has been around 827380 tons in 2014 (FAO, 2014). Eggplant is a good source of vitamins and minerals, especially in potassium and phosphorus. It contains a variety of phytochemicals such as phenolics and flavonoids (Akanitapichat et al., 2010). It is ranked amongst the top ten vegetables in terms of antioxidant capacity due to the phenolic constituents (Cao et al., 1996). Sun drying method is widely used to dry grains, vegetables, fruits and other agricultural products (İ. T. Togrul et al., 2004). In Turkey, sun drying is commonly used for drying of vegetables. In open sun drying, solar radiation directly affects the foods. The heat results in vapor formation with increasing temperature and evaporation of water from the surface of food (I. T. Togrul, 2003). During the early stages of drying, convective hot air drying is certainly the most efficient method. However, as the process continues, drying hardly progresses and slows down so it requires more energy (Argyropoulos et al., 2011). During drying process, the rate of evaporation is faster than the rate of water movement to the surface.

INTRODUCTION

Oğuzeli is center of production and sun drying of eggplant, in Gaziantep. It is one of the most famous areas that contribute in the process of drying eggplant. The eggplant is collected from the fields are cleaned by the local people. After cleaning, next step, one of the most important process, is digging Figure (1). They are left to dry on the terraces of the houses or in empty fields over the mountains under the hot sunlight and wind. It has the disadvantages of lack of control of the drying process, loss of product quality, lack of uniformity in drying, the risk of contamination by molds, bacteria, rodents, birds and insects, long drying times are dependent on climate (St George et al., 2008). Temperature and wind play an

important role in the drying process. When the temperature is high, it is being worked intensively in recent days to dry the eggplants. The duration of drying process its take 3-4 days when the temperature 30-32 C° and wind speed 18 kph (MGM) while approximately 1 and half day when temperature 40-41 C°.
They are using long rope with 2.5 meters lengths with 50 pieces of fresh eggplant Figure 2. The drying process take place in shadow region as shown as in Figure 3 and 4. Because of is exposed to heat for longer time that causes problems related to quality parameters such as unacceptable color, flavor, texture, sensory characteristics, loss of nutrients, shrinkage, reduction in bulk density and rehydration capacity Figure 5. The length of the fresh eggplant is about 7-8.3 cm while the length of dried is about 5-5.3 cm Figure 6. The thickness of digging fresh eggplant about 0.3-0.5 cm. The drying season starts at the beginning of June and ends in mid-October.

Figure 1. Sun drying process of eggplant.

Figure 2. Dried eggplant under the shadow.

Figure 3. Fresh eggplant under shadow.

Figure 4. The excess exposure to the sunlight.

Figure 5. The difference between fresh and dry eggplant in terms of length and color.

Figure 6. Thickness of digging fresh eggplant.

REFERENCES

Akanitapichat, P., et al. (2010). Antioxidant and hepatoprotective activities of five eggplant varieties. Food and Chemical Toxicology, 48(10), 3017-3021.

Argyropoulos, D., et al. (2011). Assessment of convection, hot-air combined with microwave-vacuum and freeze-drying methods for mushrooms with regard to product quality. International journal of food science & technology, 46(2), 333-342.

Cao, G., et al. (1996). Antioxidant capacity of tea and common vegetables. Journal of agricultural and food chemistry, 44(11), 3426-3431.

FAO. (2014). http://www.fao.org/faostat/en/#data/QC: Food and Agriculture Organization of United Nations.

MGM, T. C. O. v. s. İ. b. m. g. M. https://www.mgm.gov.tr/?il=Gaziantep&ilce=Oguzeli.

St George, S., et al. (2008). Dehydration processes for nutraceuticals and functional foods: Advances in Food Dehydration. 1st ed. Boca Raton: CRC Press.

Togrul, I. T. (2003). Determination of convective heat transfer coefficient of various crops under open sun drying conditions. International communications in heat and mass transfer, 30(2), 285-294.

Togrul, İ. T., et al. (2004). Modelling of thin layer drying kinetics of some fruits under open-air sun drying process. Journal of Food Engineering, 65(3), 413-425.

CONTRIBUTION OF EXTERNALLY BONDED CFRP TO THE SHEAR CAPACITY OF RC BEAMS

Karrar AL-LAMI
Wassit University
karrarali@uowasit.edu.iq

ABSTRACT: Rehabilitation of deteriorated and aged structures with fiber reinforced polymer has been proven as a successful technique due to its outstanding properties such as resistance to corrosion and high stiffness-to-weight ratio. The purpose of this study is to investigate the contribution of the externally bonded carbon fiber reinforced polymer to the shear capacity of the reinforced concrete beams. For this purpose, three reinforced concrete beams strengthened with carbon fiber reinforced polymer in form of side bonded sheet was investigated. The experimental program consisted of three beam specimens that were strengthened with carbon fiber reinforced polymer. One of the beam specimens was not reinforced with transverse steel reinforcement, while the other two were reinforced with stirrups at 200 and 100mm spacing. The strain of the transverse steel reinforcement and the externally bonded CFRP was recorded and compared. In addition, shear capacity predicted by code provisions was compared to the test results. It was indicated that the presence of the transverse steel reinforcement would reduce the contribution of the CFRP to the shear capacity. In addition, the investigated code provisions underestimate the shear capacity of the RC beams strengthened with CFRP.

Key words: CFRP, Shear strengthening, Shear capacity, FRP, Side bonding

INTRODUCTION

Fiber Reinforced Polymer (FRP) has been greatly used to strengthen deteriorated structures in the last few decades. Externally Bonded Fiber Reinforced Polymer (EB-FRP) and Near Surface Mounted (NSM) are the most popular strengthening methods. Due to its easy implementation, externally bonded strengthening technique has been widely used to increase flexural and ultimate shear capacity of Reinforced Concrete (RC) beams (Pellegrino et al. 2009, Pellegrino & Modena 2009, Chen et al. 2015, Oehlers et al. 2015, Bukhari et al 2010, Pellegrino et al. 2002, Pellegrino & Modena 2008)

Shear behavior of RC beams strengthened by EB-FRP has attracted a great attention due to its significance to prevent shear failure. Shear strengthening is performed in form of side bonding, U-wrapping, and complete wrapping. FRP can be applied in one or more than one layer. Numerous studies (Bukhari et al. 2010, Pellegrino et al. 2002, Pellegrino & Modena 2008, Pellegrino 2006, Bousselham & Chaallal 2006, Bousselham & Chaallal 2008, Pellegrino & Vasic 2013, Chen et al. 2010) made important contributions to this subject. Yet, there are still some gaps need to be filled. The contribution of the FRP to the shear capacity is one of these gaps. Design guidelines such as ACI 440.2R, fib, and CNR-DT quantify the shear

capacity of the RC beams strengthened in shear with EB-FRP by the simple sum of concrete contribution, transverse steel contribution, and FRP contribution. Nevertheless, these models sometimes lead to inaccurate assessment because they ignore the interaction between transverse steel and FRP (Pellegrino et al. 2002, Pellegrino & Modena 2008, Pellegrino 2006, Bousselham & Chaallal 2006, Bousselham & Chaallal 2008, Pellegrino & Vasic 2013, Chen et al. 2010). Therefore, more experimental tests are needed to validate these models. In this paper, the contribution of the externally bonded Carbon Fiber Reinforced Polymer (CFRP) to the shear capacity of RC beams was investigated. In addition, the shear capacity of the RC beams strengthened with CFRP obtained from the experimental program was compared with the values predicted by some code provisions.

DESIGN GUIDELINES FOR THEPREDICTION OF THE SHEAR CAPACITY

ACI 440-08

The American Concrete Institute (ACI 440.2R 2008) provisions are based on a study by Khalifa et al. (1998). Shear capacity of RC beams strengthened with FRP can be determined as follows:

$$V_{Rd} = V_c + V_s + \psi_f V_f \quad (1)$$

$$V_c = 0.17\,\lambda\sqrt{f'_c}\,b_w\,d \quad (2)$$

$$V_s = \frac{f_{wy}\,.A_{ws}\,.d}{S} \quad (3)$$

$$V_f = \frac{A_{fv}\,.f_{fe}\,.(\sin\alpha+\cos\alpha).d_f}{s_f} \quad (4)$$

$$A_{fv} = 2\,.n\,.t_f\,.w_f \quad (5)$$

$$f_{fe} = \varepsilon_{fe}\,.E_f \quad (6)$$

For complete wrapped member

$$\varepsilon_{fe} = 0.0004 \leq 0.75\,.\varepsilon_{fu} \quad (7)$$

For two or three side-bonded FRP

$$\varepsilon_{fe} = k_v\,.\,\varepsilon_{fu} \leq 0.004 \quad (8)$$

$$k_v = \frac{k_1\,.k_2\,.\,L_e}{11{,}900\,.\,\varepsilon_{fu}} \leq 0.75 \quad (9)$$

$$L_e = \frac{23{,}300}{(n\,.\,t_f\,.\,E_f)^{0.58}} \quad (10)$$

$$k_1 = \left(\frac{f'_c}{27}\right)^{2/3} \quad (11)$$

$$k_2 = \frac{d_{fv}-2\,L_e}{d_{fv}} \quad \text{For two sides bonded} \quad (12)$$

$$k_2 = \frac{d_{fv}-2\,L_e}{d_{fv}} \quad \text{For U wrapping} \quad (13)$$

Where V_c, V_s, *and* V_f are the concrete, transverse steel, and FRP contribution to the shear strength; f'_c is the compressive strength of the concrete; b_w and d are the width and the depth of the beam cross section, respectively; f_{wy} and A_{ws} are the yielding strength and cross section area of the transverse steel reinforcement; S is the spacing between transverse reinforcement; ψf is a reduction factor equals to 0.85 for two side-bonded FRP scheme and 0.95 for complete wrap scheme; A_{fv}, f_{fe},

s_f, are the FRP shear reinforcement area, effective stress and spacing respectively; a is the FRP inclination angle with respect to the longitudinal axis of the member; d_f is the FRP effective depth; E_f is the FRP tensile modulus of elasticity; ε_{fu} is the ultimate rapture strain calculated by dividing the tensile strength (f_{fu}) on the tensile modulus of elasticity (E_f); ε_{fe} is FRP effective strain at the failure point; k_v bond-reduction coefficient.

FIB 2001

The European code fib (2006) derived its model to predict the shear strength of FRP strengthened RC beams based on regression of experimental results conducted by Triantafillou & Antonopoulos (2000). The shear capacity can be determined using the following Equations:

$$V_{Rd} = \min(V_{cd} + V_{wd} + V_{fd}\ ,\ V_{Rd,2}) \quad (14)$$

$$V_{cd} = 0.9\ .\ k_v\ .\ \frac{\sqrt{f_{cm}}}{\gamma_c}\ .\ b_w\ .\ d \quad (15)$$

$$V_{wd} = 0.9\ .\ \frac{A_{sw}}{S_w}\ .\ f_{ywd}\ .\ d\ .\ (\cot\theta + \cot\beta)\sin\beta \quad (16)$$

$$V_{fd} = 0.9\ .\ \varepsilon_{fd,e}\ .\ E_{fu}\ .\ \rho_f\ .\ b_w\ .\ d\ .\ (\cot\theta + \cot\alpha).\sin\alpha \quad (17)$$

$$\varepsilon_{fd,e} = \frac{\varepsilon_{fk,e}}{\gamma_f} \quad (18)$$

$$\varepsilon_{fk,e} = k.\varepsilon_{f,e} \qquad \text{Where } \boldsymbol{k=0.8} \quad (19)$$

For fully side-bonded and U-jacketing FRP

$$\varepsilon_{f,e} = \min\left[0.65\ .\left(\frac{f_{cm}^{2/3}}{E_{fu}\cdot\ \rho_f}\right)^{0.56}\ .\ 10^{-3}\ ,\ 0.17\ .\left(\frac{f_{cm}^{2/3}}{E_{fu}\cdot\ \rho_f}\right)^{0.3}\ .\varepsilon_{fu}\right] \quad (20)$$

For continuous bonded FRP

$$\rho_f = \frac{2\ .t_f\ .\sin\alpha}{b_w} \quad (21)$$

For FRP sheet or strips of width b_w at spacing s_f:

$$\rho_f = \left(\frac{2\ .\ t_f}{b_w}\right)\ .\left(\frac{b_f}{s_f}\right) \quad (22)$$

Where V_{cd} and V_{wd} are the concrete and transverse steel contribution to the shear strength, respectively; V_{fd} is the FRP contribution; k_v is a model parameter defined by the levels of approximation and represents the ability of the web to resist aggregate interlock stresses (fib 2010); γ_c is a partial safety factor for concrete; f_{ywd}, A_{sw} is the yielding strength and cross section area of the transverse steel, respectively; s_w is the spacing between transverse steel; γ_f is the partial safety factor which is 1.30 for the bonding failure; $\varepsilon_{fd,e}$ design value of the effective FRP strain; ε_{fu} is the FRP ultimate strain; E_{fu} modules of elasticity for the FRP in the principal fiber orientation in GPa; f_{cm} is the cylindrical compressive strength of concrete in MPa; ρ_f is the FRP reinforcement ratio; d and b_w are the depth and the width of the cross section, respectively; a is the angle between the longitudinal axis of the member and principal fiber orientation; θ is the angle of the diagonal crack with respect to the member axis (assumed 45); β is the angle between transverse steel reinforcement and longitudinal axis of the member.

CNR-DT200 (2013)

The Italian CNR-DT proposed the following expression to determine the shear capacity of the RC beams strengthened by externally bonded FRP:

$$V_{Rd} = \min\left[V_{Rd,s} + V_{Rd,f};\ V_{Rd,c}\right] \quad (23)$$

For FRP side bonding configuration

$$V_{Rd,f} = \frac{1}{\gamma_{Rd}} . 0.9 . d . f_{fed} . 2 . t_f . (\cot\theta + \cot\beta) . \frac{b_f}{p_f} \quad (24)$$

Where $V_{Rd,s}$, and $V_{Rd,f}$ are the steel and FRP contributions to the shear capacity, respectively; $V_{Rd,c}$ is the maximum shear force the section can resist before crashing of the concrete in the compression zone; f_{fed} is the FRP effective design strength; b_f and p_f are the FRP width and spacing, respectively, measured orthogonally to the fiber direction (for FRP strips installed one next to each other, the ratio of b_f/p_f equals to 1.0); γ_{Rd} is a partial factor for resistance models (For shear and torsion, its value equals 1.20); β is the angle between the FRP sheet and the longitudinal axis; θ is the angle of the shear crack (assume equals to 45° unless more calculations are made).

$$f_{fed} = f_{fdd}\left[1 - \frac{1}{3} . \frac{l_{ed} . \sin\beta}{\min[0.9d; h_w]}\right] \quad (25)$$

$$f_{fdd} = \frac{1}{\gamma_{f,d}} \sqrt{\frac{2 . E_f . \Gamma_{Fd}}{t_f}} \quad (26)$$

$$l_{ed} = \frac{1}{\gamma_{Rd} . f_{bd}} \sqrt{\frac{\pi^2 . E_f . t_f . \Gamma_{Fd}}{2}} \quad (27)$$

$$f_{bd} = \frac{2 . \Gamma_{Fd}}{s_u} \quad (28)$$

(s_u = 0.25mm is the design bond strength between FRP and concrete)

Where h_w is the cross section depth; f_{fdd} is the design debonding strength of FRP; l_{ed} is the effective bond length; $\gamma_{f,d}$ is partial factor ranged between 1.20 to 1.50; E_f and t_f are the FRP modules of elasticity and thickness, respectively. For effective bond length evaluation, γ_{Rd} equals to 1.25. Γ_{Fd} is the design value of the specific fracture energy which can be determined as follows:

$$\Gamma_{Fd} = \frac{k_b . k_G}{FC} . \sqrt{f_{cm} . f_{ctm}} \quad (29)$$

$$k_b = \sqrt{\frac{2 - \frac{b_f}{b}}{1 + \frac{b_f}{b}}} \geq 1.0 \quad (30)$$

Where f_{ctm} is the concrete average tensile strength; f_{cm} is the concrete compressive strength; FC is a confident factor (assumed 1.0); k_G is a corrective factor equal to 0.023mm or 0.037mm for pre-cured and wet lay-up schemes, respectively. k_b is the geometric coefficient factor depending on both of the strengthened beam and FRP. The following points should be considered when calculating k_b value:

* $b = p_f$ for discrete FRP strip application

* $b = b_f = \min[0.9d;\ h_w] . \frac{\sin(\theta+\beta)}{\sin\theta}$ For FRP system installed continuously along the length

EXPERIMENTAL PROGRAM

Specimen and Material

The experimental program consisted of three rectangular RC beam specimens. They were designed such that their ultimate shear capacity was reached before their ultimate flexural capacity as shown in Table 1. Except for specimen B1 that did not have transverse steel reinforcement, the other two beams were reinforced with transverse steel reinforcement at 100mm and 200mm spacing. The specimens were cast in the laboratories of the Civil Engineering Department of Wasit University using an electric mixer of 0.15 m^3. The properties of the concrete were as follows: cement = 412 kg/m^3, fine aggregate = 648 kg/m^3, coarse aggregate = 1152 kg/m^3, and water-cement ratio (w/c) = 0.45. Cylindrical specimens of 150 mm diameter and 300 mm length were used to determine the compressive strength. The mean compressive strength at the age of 28 days was 23.5 MPa.

Table 1. Details of Specimens

Specimen	*b* (mm)	*d* (mm)	a/d	Tension Steel	ρ	Compression steel	Stirrups diameter (mm)	Stirrups spacing, (mm)
B1	150	200	2.75	2ϕ25 mm	0.041	2ϕ10 mm	N/A	N/A
B2	150	200	2.75	2ϕ25 mm	0.041	2ϕ10 mm	6	200
B3	150	200	2.75	2ϕ25 mm	0.041	2ϕ10 mm	6	100

Strengthening Procedure

All beam specimens were strengthened with side-bonded CFRP sheets along the entire length of the beams as shown in Figure 1. First, concrete surface was prepared using a grinder and sand paper. Then, it was cleaned with a wet piece of cloth to remove all the remaining dust. Finally, one layer of unidirectional Sika-Wrap-301C carbon fabric was applied using Sikadur- 330 impregnating resin as an adhesive. Table 2 shows the geometric and mechanical properties of the CFRP.

Table 2. Geometric and Mechanical Properties of the CFRP

Type	Width (mm)	Thickness (mm)	Tensile strength (MPa)	Tensile modules of elasticity (MPa)	Elongation at break %
Sika-Wrap-301C	500	0.167	4,900	230,000	1.7

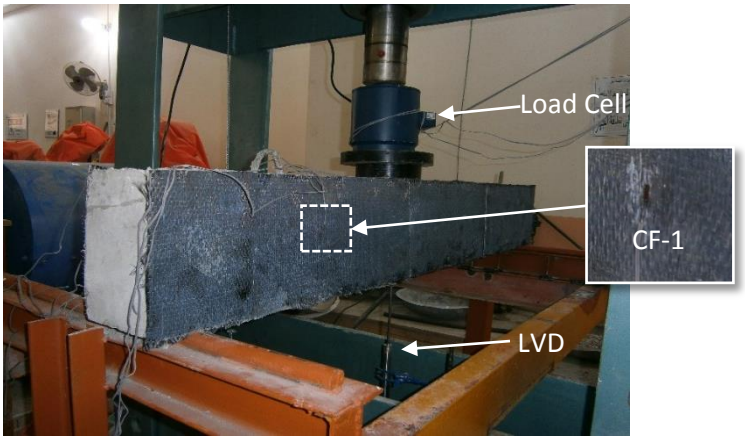

Figure 1. Test Setup

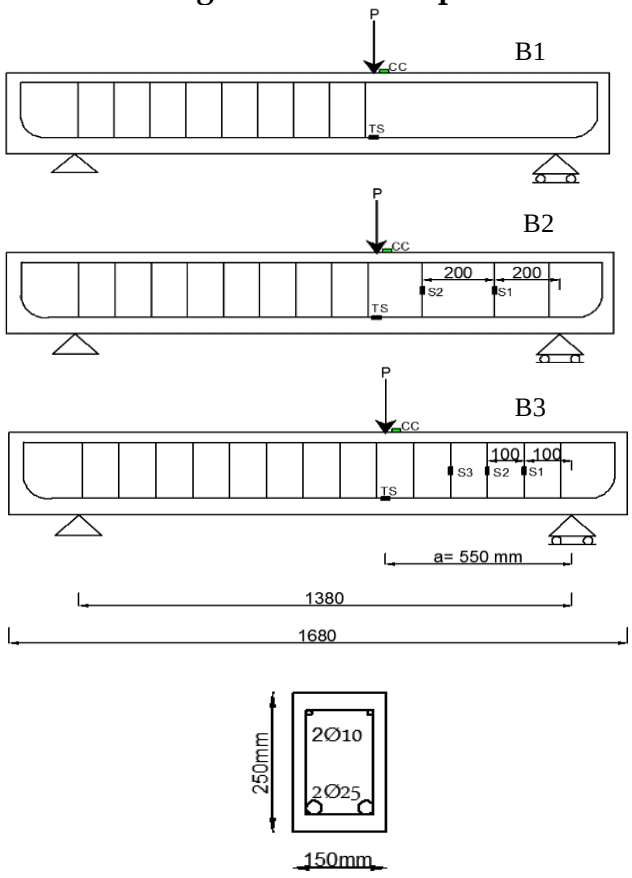

Figure 2. Specimens' Details and Instruments Position

Test Setup and Instruments

Simply supported scheme with three-point loading was carried out in this study as shown in Figure 1 and 2. Signals from the instruments were monitored and recorded by an automatic data acquisition system. The load was applied using 500 kN hydraulic jack with manual control. The applied load was measured using load cell of 1000 kN capacity. The deflection of the beam beneath the point of the applied load was captured with Linear Variable Displacement Transducer (LVDT). Two strain gauges, CF-1 and CF-2, located at 250 mm from the support

were used to measure the strain of the CFRP on the both sides of the beam as shown in Figure 1. Waterproof strain gauges were used to measure the strain in the stirrups as shown in Figure 2. Strain gauges, TS and CC, were also used to measure the strain at the tensile steel reinforcement and compression concrete, respectively.

RESULTS AND DISCUSSIONS

Load-Deflection Relationship

Load-deflection relationship was utilized to assess the enhancement of the shear capacity of the RC beams strengthened with the CFRP. The load-deflection relationship obtained from the experimental program is presented in Figure 3. It can be noticed a brittle failure developed in specimen B1at a load of 160.0 kN due to the absence of the transverse steel reinforcement. However, a ductile failure was developed in specimens B2 and B3 due to the presence of the internal transverse shear reinforcement at a load of 164.9 kN and 254.9 kN respectively.

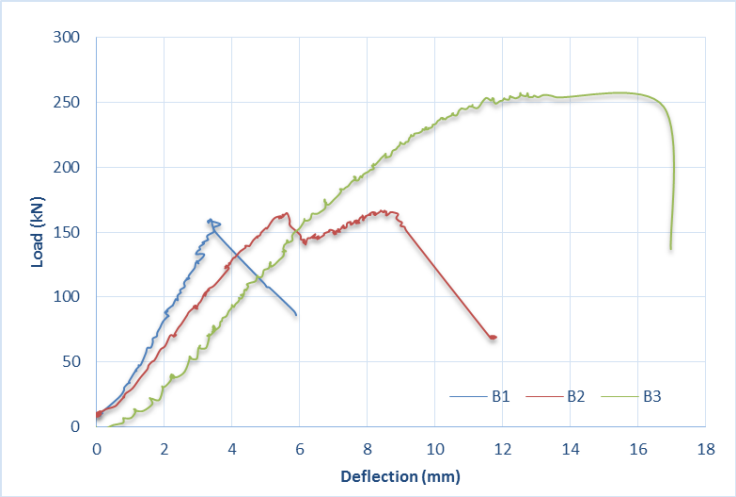

Figure 3. Load-Deflection Curves

All the beams failed by shear with CFRP delamination. First diagonal shear crack initiated at the point of the applied load then it was propagated toward the closest support. After that, CFRP delamination, combined with a small layer of concrete, was developed at the top and the bottom of the beams as shown in Figure 4. Finally, CFRP debonding propagated toward the inclined shear crack causing beams' failure.

Strain Comparison

Strain developed in the CFRP within the shear span was measured by two strain gauges (CF-1, and CF-2) placed on both faces of each specimen and located at 250 mm from the support. Figure 5 compares between the strains developed within the three specimens. It can be observed that though the shear capacity of specimen B1 is almost equal to B2, CFRP in B1 was more strained than B2. This result attributed to the higher contribution of the CFRP in the case of B1 due to the absence of the transverse steel reinforcement. In other words, since specimen B1 was not reinforced with transverse steel, its CFRP contribution to the shear strength was higher. For specimen B3, shear capacity was increased by decreasing the spacing between transverse steel reinforcement within the shear span. However, the strain captured in the CFRP at the failure was almost equal to the one captured in B2 indicating that the presence of transverse steel reinforcement can reduce CFRP contribution to a constant value.

Figure 4. Failure Mode

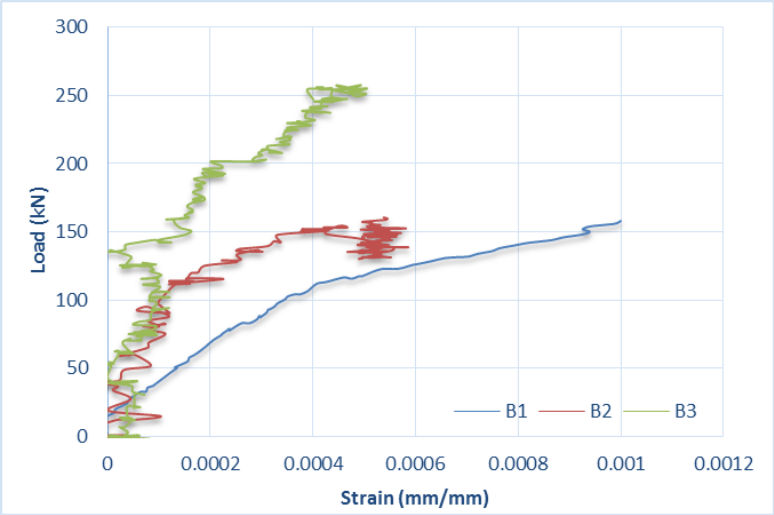

Figure 5. Load-Strain of the Three Specimens

Figure 6 compares between strains measured by S1, S2, and CF-1 for specimen B3. Results highlighted that strains developed in both stirrups were higher than the one developed in the CFRP. This result supports the finding obtained earlier that CFRP contribution to the shear capacity of beam reinforced with transverse steel would be lower than the unreinforced one.

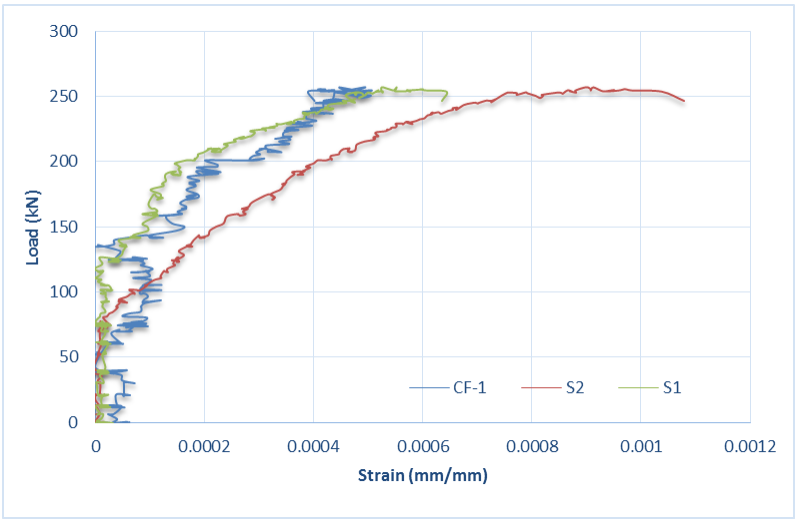

Figure 6. Load-Strain of Specimen B3

Comparison between measured shear capacity and predicted shear capacity

Shear capacity obtained from the experimental program was compared to the one predicted by code provisions in Table 3. From the comparison, it can be detected that code provisions had conservative predictions for the shear capacity of the RC beams strengthened with CFRP. The ACI 440-08 had the closest predictions, especially for specimen B2. However, the CNR-DT had the most conservative

predictions, especially for specimen B1. This result can be attributed to the fact that CNR-DT neglect the contribution of the concrete to the shear capacity. Based on that, shear capacity of specimen B1 represents the contribution of the CFRP component only. This comparison proves that some expression adopted by design guidelines need to be improved more.

Table 3. Comparison between Measured Shear Capacity and Predicted Shear Capacity

		Shear capacity (V_{Rd}) MPa		
		B1	B2	B3
Experimental results $V_{Rd, exp.}$		160.0	164.9	254.9
Code predictions $V_{Rd, code}$	ACI 440-08	82.3	121.7	161.2
	fib	66.1	100.3	135.8
	CNR-DT	41.5	77.0	112.4
$V_{Rd, exp}/ V_{Rd, code}$	ACI 440-08	2.0	1.4	1.6
	fib	2.4	1.6	1.9
	CNR-DT	3.9	2.1	2.3

CONCLUSION

In this paper, the interaction between the transverse steel reinforcement and the externally bonded CFRP was investigated. The experimental results showed that using CFRP in conjunction with transverse steel reinforcement shifted failure mode from a brittle failure to a ductile failure. Moreover, the strain developed in the externally bonded CFRP was reduced, which indicates a lower contribution to the shear capacity. Comparing shear capacity estimated by code provisions with the test results indicated that the current code provisions have a conservative prediction formulas, especially the CNR-DT (2013). Therefore, more studies are advised to have more accurate models.

REFERENCES

ACI committee 440. (2008). *Guide for the design and construction of externally bonded FRP systems for strengthening existing structures. ACI committee 440.*
ACI 440.2R-02 2011. *Guide for the design and construction of externally bonded FRP systems for strengthening concrete structures*. Farmington Hills, USA: American Concrete Institute.
Bousselham, A., & Chaallal, O. (2006). Behavior of reinforced concrete T-beams

strengthened in shear with carbon fiber-reinforced polymer-an experimental study. *ACI Structural Journal*, *103*(3), 339.
Bousselham, A., & Chaallal, O. (2008). Mechanisms of shear resistance of concrete beams strengthened in shear with externally bonded FRP. *Journal of Composites for Construction*, *12*(5), 499–512.
Bukhari, I. A., Vollum, R. L., Ahmad, S., & Sagaseta, J. (2010). Shear strengthening of reinforced concrete beams with CFRP. *Magazine of Concrete Research*, *62*(1), 65–77.
Chen, G. M., Teng, J. G., Chen, J. F., & Rosenboom, O. A. (2010). Interaction between Steel Stirrups and Shear-Strengthening FRP Strips in RC Beams. *Journal of Composites for Construction*, *14*(5), 498–509.
Chen, G. M., Teng, J. G., Chen, J. F., & Xiao, Q. G. (2015). Finite element modeling of debonding failures in FRP-strengthened RC beams: A dynamic approach. *Computers and Structures*, *158*, 167–183.
CNR-Italian Research Council, Advisory Committee on Technical Recommendations for Construction, 2013, Guide for the Design and Construction of Externally Bonded FRP Systems for Strengthening Existing Structures. Materials, RC and PC Structures, Masonry Structures (CNR-DT 200/2013). Rome, Italy.
Fédération Internationale du Béton (fib)(2010): Shear and punching shear in RC and FRC elements, fib Bulletin 57.
Fédération Internationale du Béton (fib) (2001). Externally bonded FRP reinforcement for RC structures. Task Group 9.3, Bullettin No. 14, Lausanne,Switzerland.
Khalifa, A., Gold, W., Nanni, A. & Abdel Aziz, M. I. 1998. Contribution of externally bonded FRP to shear capacity of RC flexural members. Journal of Composites for Construction 2(4): 195-202.
Oehlers, D. J., Visintin, P., & Lucas, W. (2015). Flexural strength and ductility of FRP-plated RC beams: Fundamental mechanics incorporating local and global IC debonding. *Journal of Composites for Construction*, *20*(2), 4015046.
pellegrino, C, and M. (2006). Fiber-reinforced polymer shear strengthening of reinforced concrete beams: Experimental study and analytical modeling. *ACI Structural Journal*, *15*(5), 720–728.
Pellegrino, C., Maiorana, E., & Modena, C. (2009). FRP strengthening of steel and steel-concrete composite structures: an analytical approach. *Materials and Structures*, *42*(3), 353–363.
Pellegrino, C., & Modena, C. (2008). An experimentally based analytical model for the shear capacity of FRP-strengthened reinforced concrete beams. *Mechanics of Composite Materials*, *44*(3), 231–244.
Pellegrino, C., & Modena, C. (2009). Flexural strengthening of real-scale RC and PRC beams with end-anchored pretensioned FRP laminates. *ACI Structural Journal*, *106*(3), 319.
Pellegrino, C., Modena, C., & pellegrino, C, and M. (2002). Fiber reinforced polymer shear strengthening of reinforced concrete beams with transverse steel reinforcement. *Journal of Composites for Construction*, *6*(2), 104–111.

Pellegrino, C., & Vasic, M. (2013). Assessment of design procedures for the use of externally bonded FRP composites in shear strengthening of reinforced concrete beams. *Composites Part B: Engineering*, *45*(1), 727–741.

AERODYNAMIC ANALYSIS OF A RC AIRPLANE

İbrahim GÖV
Gaziantep University
igov@gantep.edu.tr

Abstract: In this study, lift force and drag force of a RC airplane was calculated using computational fluid dynamic (CFD) analysis. NACA 2412 airfoil was used for wing design. When the aircraft is moving into the air, it subjects to aerodynamic forces. These aerodynamic forces are the drag, lift, and thrust forces. Drag force produces a resistant to relative motion. Lift is the force that directly opposes the weight of an airplane and holds the airplane in the air. Thrust is generated by the engines of the aircraft through some kind of propulsion system. Drag and lift forces were investigated at maximum speed to represent the aerodynamic performance of a RC airplane.

Key words: RC airplane, Aerodynamic analysis, Drag force, Lift force.

INTRODUCTION

In the design stage of airplanes, aerodynamic analysis is very important step of the design. After performing the aerodynamic analysis, lift force and drag force values are determined. Lift force must be maximized and drag force must be minimized to increase fuel efficiency. In the literature, many different studies are existing due to the aircrafts. Some of them are related to structural parts, hydraulic systems and brake systems analysis. Some of them are associated with fatigue, aerodynamic and dynamic behavior.

Hedges et. al. (2002) studied on the flow around a generic airliner landing gear truck using the methods of Detached-Eddy Simulation, and of Unsteady Reynolds-Averaged Navier-Stokes Equations, with the Spalart-Allmaras one-equation model. Comparison of experimental and calculated results is performed. It is seen that simulation can give the pressure of wheels correctly.

A general aviation airplane was designed and analyzed. A three-dimensional layout of the airplane was created using RDS software based on conic lofting. Static stress analysis was performed for wing design purposes. Using the finite element software package COMSOL, the calculated aerodynamic loads were applied to the wing to check the wing reliability (Atmeh et al., 2010).

A wing is a surface used to produce an aerodynamic force normal to the direction of motion by traveling in air or another gaseous medium. A wing is an extremely efficient device for generating lift. Its aerodynamic quality, expressed as a Lift-to-drag ratio, can be up to 60 on some gliders and even more. This means that a significantly smaller thrust force can be applied to propel the wing through the air

in order to obtain a specified lift (Chitte et al., 2013). So, in the literature many different study is exist about the aerodynamic force analysis.

Doğru and Güzelbey (2014) studied on static thrust calculation of ducted fan in various speeds. They used two experimental method to obtain static thrust. In the first method, the duct fan was placed in the pipe regarding to drill some static tapping holes on the pipe. Static pressure was measured and the thrust of the duct fan has been obtained from this measurement. In the second method, a spring system was established for getting duct fan thrust force.

A landing gear is designed by using CAD software and structural safety for static and spectrum loads is analyzed using ANSYS by Imrana et. al. (2015). The maximum possible loads applied through RBE3 connection at the axle end spreading to wheel base. The composite material is used to check the strength of the landing gear for self-weight, static loads, modal conditions and shock spectrum loads as per mil standards. The results show lesser stresses and deflections with composite material.

Doğru et. al. (2016) investigated the static thrust analysis by experimentally. The static thrust value was obtained experimentally under the effect of the ducted fan, which is located inside the ground effect region. The thrust of the ducted fan was measured using two different experimental methods. In the first method, the static pressure measurement system was used to calculate the thrust. The spring method was used in the second method to calculate the thrust. They obtained that the lift force decreased, as expected.

Velocity distribution and turbulence energy were investigated for the projectiles on different tip shapes by using SolidWorks Flow Simulation CFD analysis. Three different projectile nose shapes were examined in the study. Initial velocity was accepted to be 500 m/s for all situations. At the end of the study, velocity and pressure distribution on the penetrators in different tip geometries were obtained. The maximum velocity decrease at the tip of penetrator was found to be as 57.5% for the rounded type projectile (Doğru, 2017).

At the end of the literature survey, it is seen that many studies exist related with airplanes. Such as analysis of the hydraulic systems, brake systems and structural parts were performed. Lift force and drag force values are very critic specification for fuel efficiency of an airplane. So, this study concentrated on aerodynamic analysis of a RC airplane to calculate lift force and drag force.

ANALYSES

All analyses are performed using SolidWorks Flow Simulation program. Drag force and lift force on a RC airplane (in figure 1) are obtained by using aerodynamic analyses. NACA 2412 airfoil (in figure 2) is used for wing design. Cruse speed is taken as 30 m/s and angle of attack is taken as 0^0, 5^0, 10^0, 15^0, and 20^0.

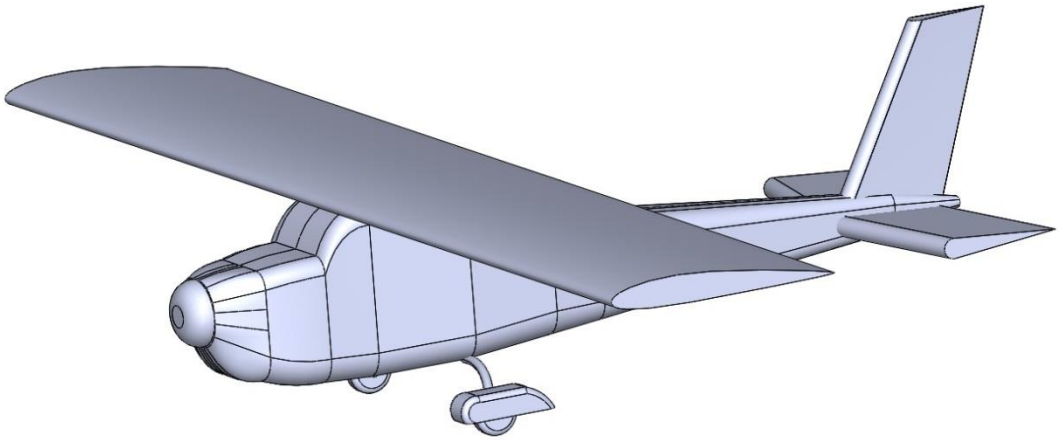

Figure 1. Solid Model of Airplane (Adiwibowo B., 2013)

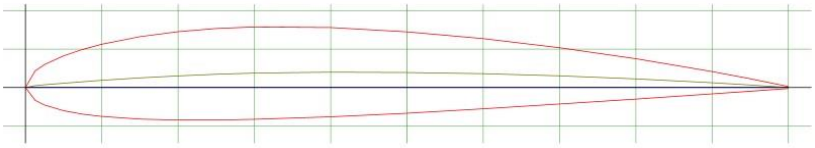

Figure 2. NACA 2412 Airfoil (AirfoilTools, 2017)

RESULTS

Flow trajectories of velocity and pressure at 0^0 AoA on airplane are given in figure 3 and figure 4 respectively.

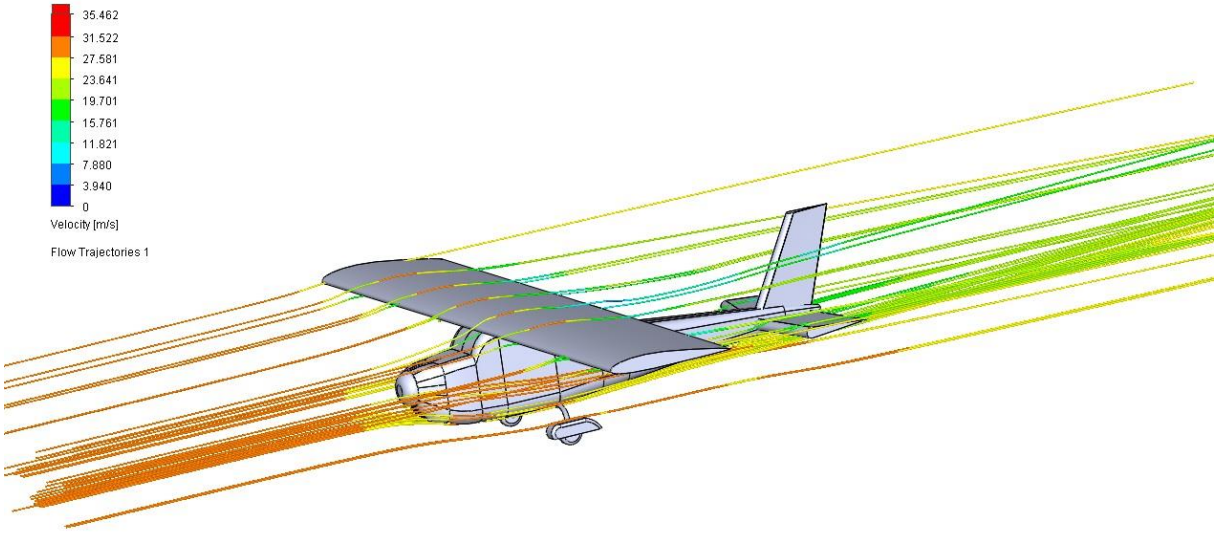

Figure 3. Flow Trajectories of Velocity on Airplane at 0^0 AoA

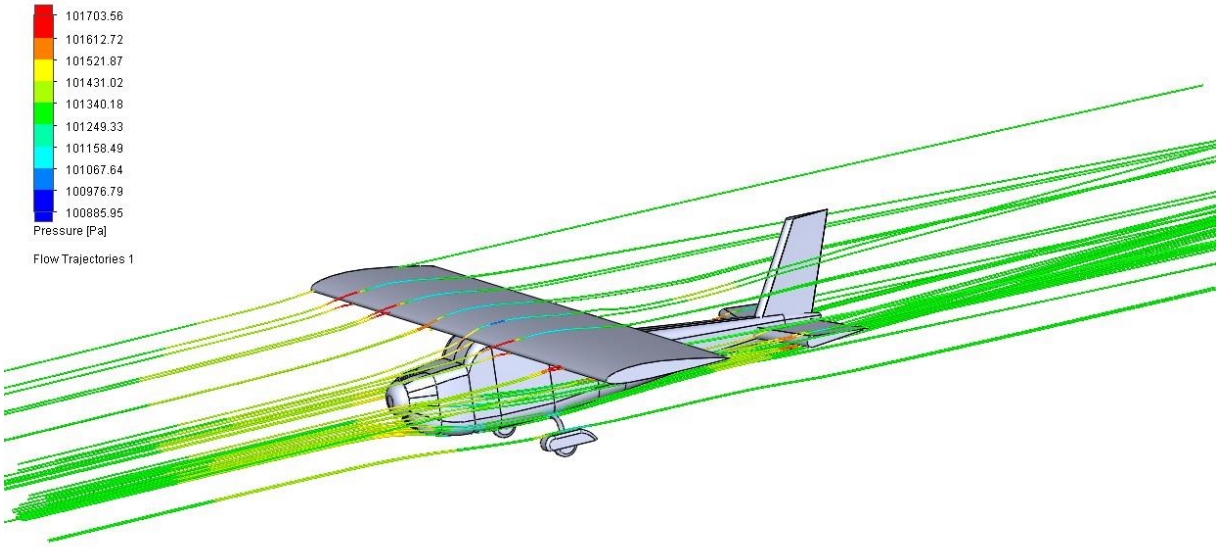

Figure 4. Flow Trajectories of Pressure on Airplane at 0^0 AoA

Flow trajectories of velocity and pressure at 5^0 AoA on airplane are given in figure 5 and figure 6 respectively.

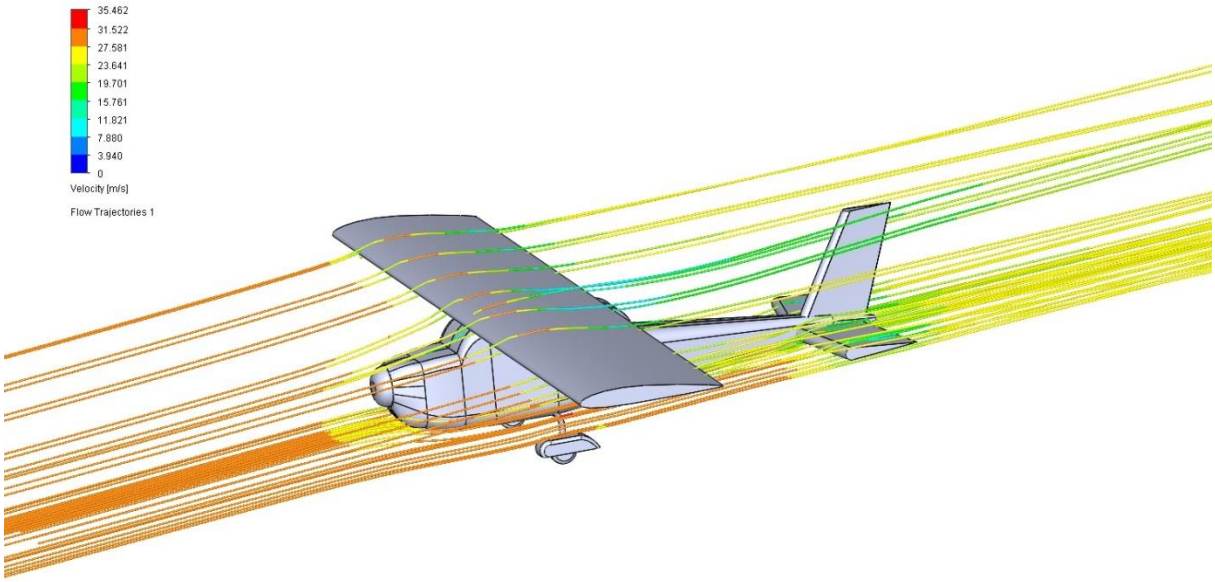

Figure 5. Flow Trajectories of Velocity on Airplane at 5^0 AoA

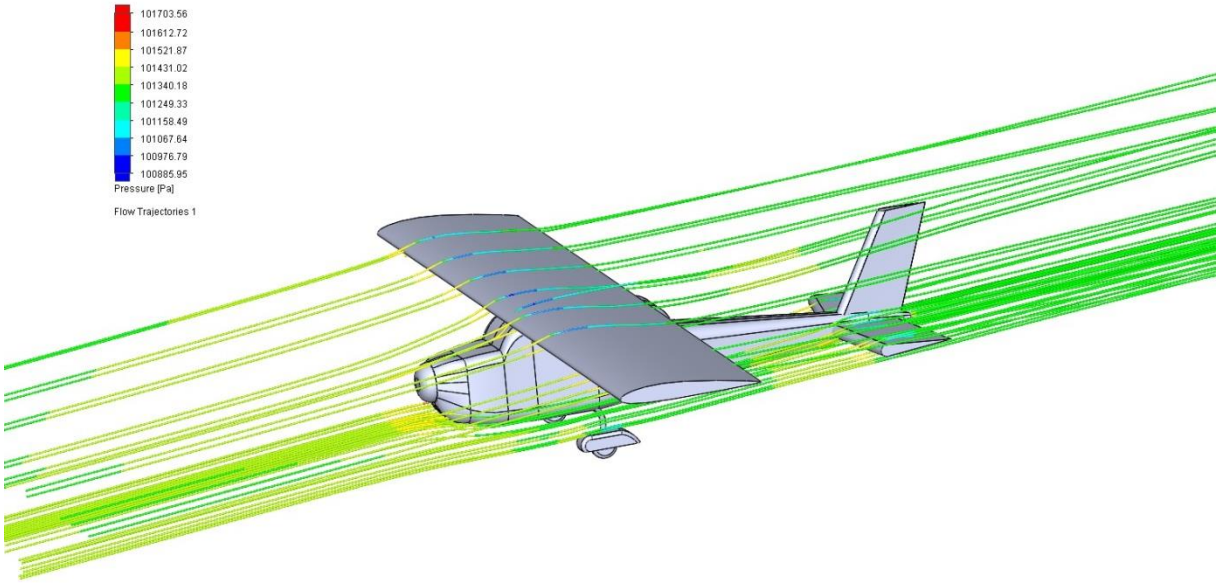

Figure 6. Flow Trajectories of Pressure on Airplane at 5^0 AoA

Flow trajectories of velocity and pressure at 10^0 AoA on airplane are given in figure 7 and figure 8 respectively.

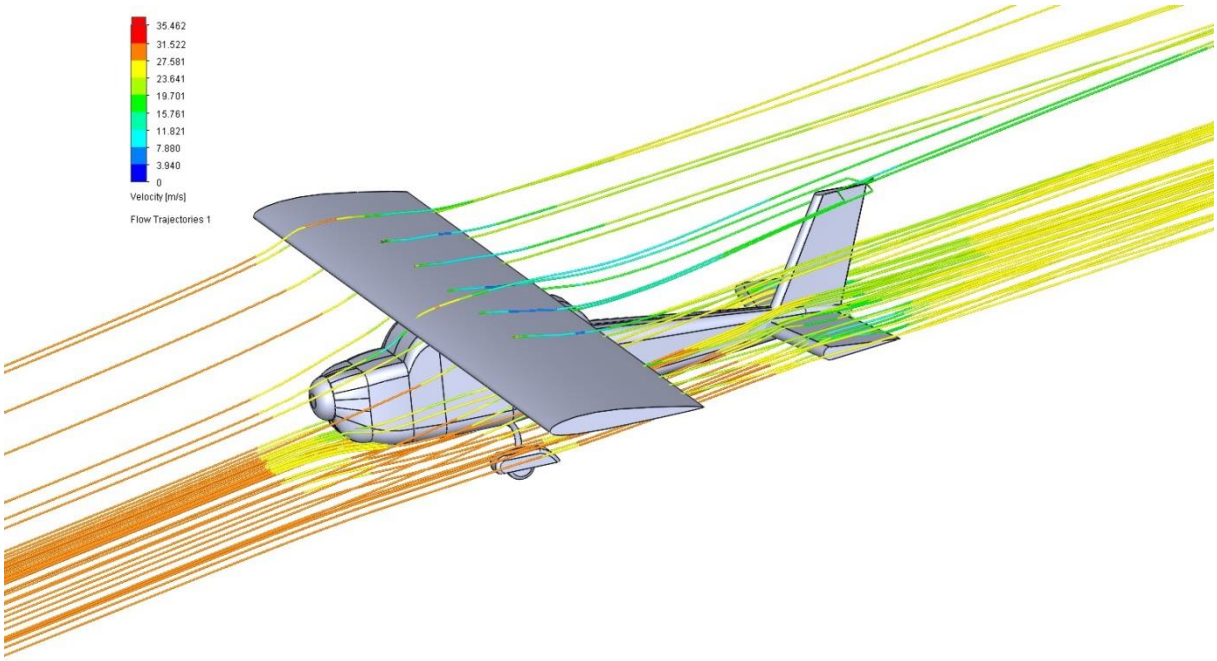

Figure 7. Flow Trajectories of Velocity on Airplane at 10^0 AoA

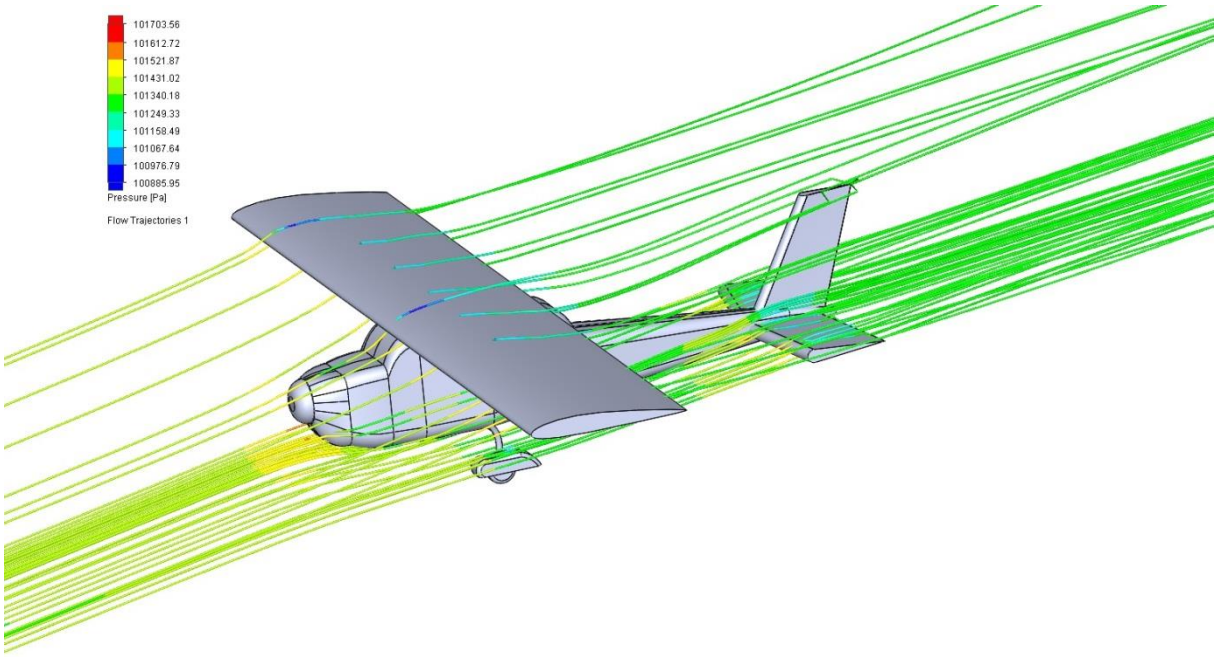

Figure 8. Flow Trajectories of Pressure on Airplane at 10^0 AoA

Flow trajectories of velocity and pressure at 15^0 AoA on airplane are given in figure 9 and figure 10 respectively.

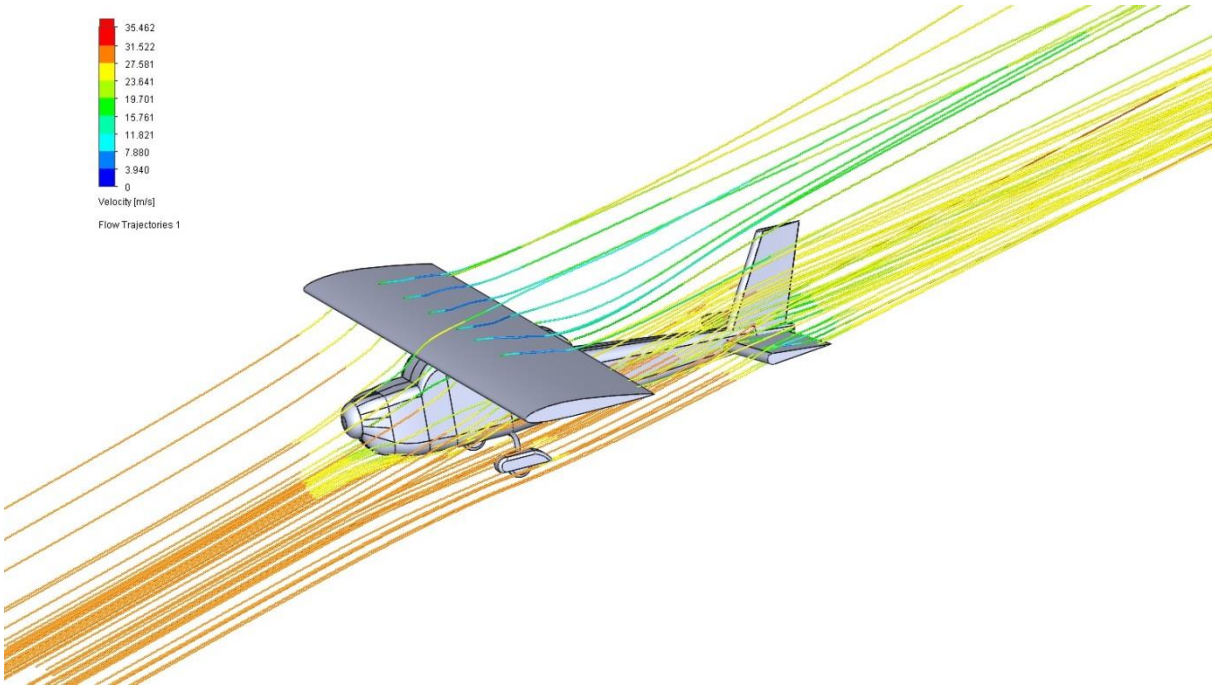

Figure 9. Flow Trajectories of Velocity on Airplane at 15^0 AoA

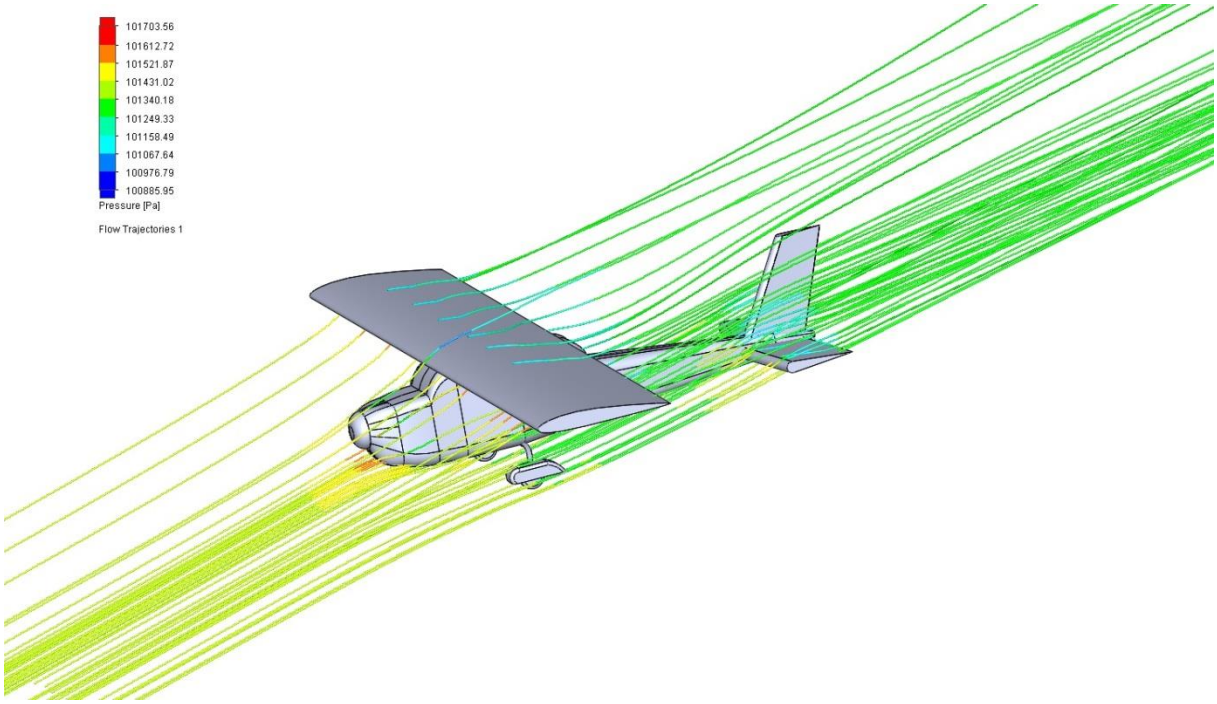

Figure 10. Flow Trajectories of Pressure on Airplane at 15^0 AoA

Flow trajectories of velocity and pressure at 20^0 AoA on airplane are given in figure 11 and figure 12 respectively.

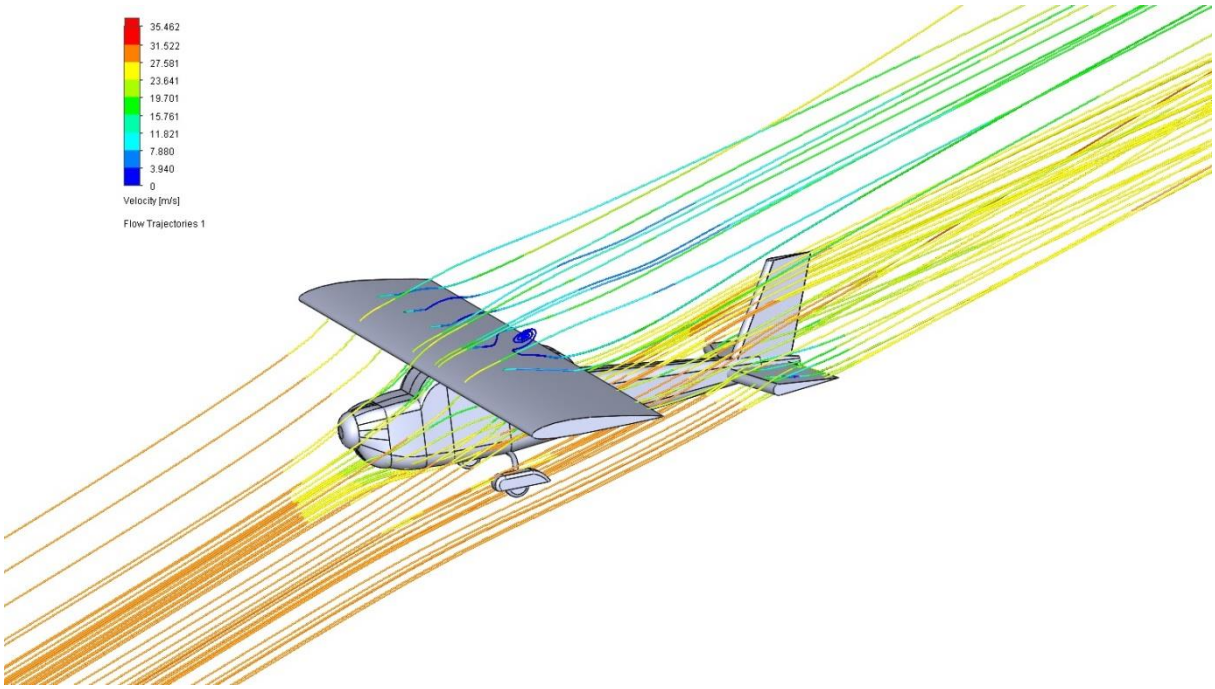

Figure 11. Flow Trajectories of Velocity on Airplane at 20^0 AoA

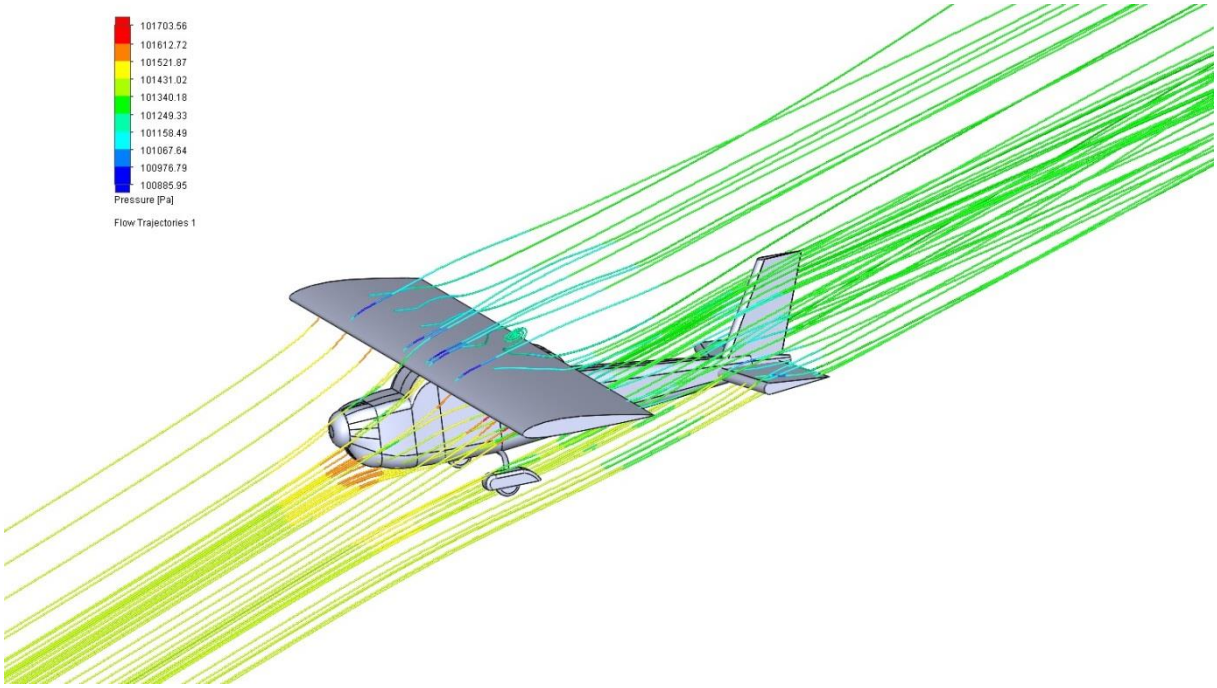

Figure 12. Flow Trajectories of Pressure on Airplane at 20^0 AoA

Lift force and drag force results at different angle of attack values are listed in table 1.

Table 1 Lift and Drag Force Results

	Lift Force (N)	**Drag Force (N)**
0^0 AoA	20	11,8
5^0 AoA	47,7	12,7
10^0 AoA	76,6	13,2
15^0 AoA	97,4	13,8
20^0 AoA	114,8	13,9

When the result which are given in table 1 are compared, drag force and lift force values are increased due to AoA increment.

CONCLUSION

Lift force and drag force of a RC airplane is calculated using computational fluid dynamic (CFD) analysis. NACA 2412 airfoil is used for wing design. Flow trajectories of velocity and pressure on airplane are given at different AoA values (0^0, 5^0, 10^0, 15^0, and 20^0). After this study, it is shown that both drag force and lift force values are increased due to AoA increment.

REFERENCES

Adiwibowo B., (2013). Retrieved from https://grabcad.com/library/cessna-172--1.

AirfoilTools, (2017). Retrieved from http://airfoiltools.com/airfoil/details?airfoil=naca2412-il.

Atmeh G.M., Hasan Z., Darwish F., 2010. Design and stress analysis of a general aviation aircraft wing. *COMSOL Conference*, Boston.

Chitte P., Jadhav P.K., Bansode S.S., 2013. Statistic and dynamic analysis of typical wing structure of aircraft using Nastran. International Journal of Application or Innovation in Engineering & Management (IJAIEM) 2, 7.

Doğru M.H., (2017). Investigation of Velocity Distribution and Turbulent Energy for the Different Tip Shaped Projectiles. *Çukurova University Journal of the Faculty of Engineering and Architecture*, In Press.

Doğru, M. H., Güzelbey İ. H., (2014). Kanal Fanının İtme Kuvvetinin Deneysel Olarak Hesaplanması. *Makina tasarım ve imalat dergisi*, 14(1).

Doğru, M. H., İ. H. Güzelbey, and Göv İ., (2016). Ducted Fan Effect on the Elevation of a Concept Helicopter When the Ducted Faintail Is Located in a Ground Effect Region. *Journal of Aerospace Engineering*, DOI: 10.1061/(ASCE)AS.1943-5525.0000519.

Hedges, L. S., Travin, A. K., Spalart, P. R., (2002). Detached-Eddy Simulations over a Simplified Landing Gear. *Journal of Fluids Engineering*, 124.

Imrana, M.,Shabbir, A.R.M, Haneefe M., (2015). FE Analysis for Landing Gear of Test Air Craft. *Materials Today: Proceedings*, 2, 2170 – 2178.